HHS Public Access

Author manuscript

Mitochondrion. Author manuscript; available in PMC 2021 September 01.

Published in final edited form as:

Mitochondrion. 2020 September ; 54: 102–112. doi:10.1016/j.mito.2020.08.002.

Characterization and origins of cell-free mitochondria in healthy murine and human blood

Olivia R. Stephens[1], **Dillon Grant**[1], **Matthew Frimel**[1], **Nicholas Wanner**[1], **Mei Yin**[2], **Belinda Willard**[3], **Serpil C. Erzurum**[1], **Kewal Asosingh**[1,4,*]

[1]Department of Inflammation and Immunity, Cleveland Clinic, Cleveland, OH.

[2]Department of Imaging Core, Cleveland Clinic, Cleveland, OH.

[3]Department of Proteomics and Metabolomics Core, Cleveland Clinic, Cleveland, OH.

[4]Department of Flow Cytometry Core Lerner Research Institute, Cleveland Clinic, Cleveland, OH.

Abstract

Intact cell-free mitochondria have been reported in microparticles (MPs) in murine and human bodily fluids under disease conditions. However, cellular origins of circulating extracellular mitochondria have not been characterized. We hypothesize that intact, cell-free mitochondria from heterogeneous cellular sources are present in the circulation under physiological conditions. To test this, circulating MPs were analyzed using flow cytometry and proteomics. Murine and human platelet-depleted plasma showed a cluster of MPs positive for the mitochondrial probe MitoTracker. Transgenic mice expressing mitochondrial-GFP showed GFP positivity in plasma MPs. Murine and human mitochondria-containing MPs were positive for the platelet marker CD41 and the endothelial cell marker CD144, while hematopoietic CD45 labeling was low. Both murine and human circulating cell-free mitochondria maintained a transmembrane potential. Circulating mitochondria were able to enter rho-zero cells, and were visualized using immunoelectron microscopic imaging. Proteomics analysis identified mitochondria specific and extracellular vesicle associated proteins in sorted circulating cell-free human mitochondria. Together the data provide multiple lines of evidence that intact and functional mitochondria originating from several cell types are present in the blood circulation.

Keywords

Mitochondria; microparticles; extracellular vesicles; circulation

*Corresponding author: Kewal Asosingh, asosink@ccf.org, Tel. (216)444-0891, Address: 9500 Euclid Ave, NB20, Cleveland, OH 44195.

DISCLOSURES

The authors declare that they have no conflicts of interest with the contents of this article.

INTRODUCTION

Microparticles (MPs) are membrane enclosed particles that are released from various cells types (1–3). They are important mediators of intercellular trafficking. Often they contain cellular components such as DNA, microRNA, mRNA, cytokines, functional enzymes, or mitochondrial components (4–8). These components can be transferred to other cells, modulating their function (4,5,9). MPs have been implicated in regulation of many physiological processes such as angiogenesis (10), coagulation (11,12), innate immunity (13), adaptive immunity (14), and tissue repair (15). Due to their ability to modulate cellular function and their role in intercellular communication, MPs have been implicated as a biomarker in many disease states such as cancer, asthma, metabolic syndrome, arthritis, pulmonary arterial hypertension, and cardiovascular disease (16–21).

Recent work demonstrates MPs can contain not only mitochondrial components, but intact mitochondria as well (22,23). Extracellular mitochondrial components are well described mediators of inflammation. Mitochondrial DNA (mtDNA) and formyl peptides released from injured cells activate an innate immune response that induces a sepsis-like state (24). Cells undergoing apoptosis or necrosis release intact mitochondria that activate inflammatory responses *in vitro* (25,26). Similarly, activated platelets release both free and MP-encapsulated mitochondria *in vitro* which promote leukocyte activation (22). Interestingly, these mitochondria consume oxygen, suggesting they are respiratory competent. *In vivo*, intact mitochondria have been detected in synovial fluid from rheumatoid arthritis patients (22), bronchoalveolar lavage (BAL) fluid from injured mouse lungs (22), plasma from mice with traumatic brain injuries (27), and plasma from deceased organ donors (28). Together these results suggest release of intact mitochondria occurs in response to cellular stress or damage. One study, however, detected MPs containing intact mitochondria in BAL from both healthy and asthmatic humans (23), demonstrating that release of whole mitochondria also occurs in the absence of pathological stimuli.

While intact mitochondria have been detected in plasma under pathological conditions (27,28), cell-free mitochondria and their cellular sources have not been studied in the circulation of healthy individuals. Here we used flow cytometry to detect circulating mitochondria in platelet-depleted plasma in healthy mice and humans. We demonstrate that these mitochondria have platelet-, endothelial-, and leukocyte-specific surface markers suggesting they originated from these cells. Furthermore, circulating cell-free mitochondria have an active transmembrane potential and were able to enter rho-zero cells.

MATERIALS AND METHODS

Mice

10 week old C57/BL6 wildtype (WT) mice (n=5 female, n=5 male) were used for MP surface marker staining. GFP-mito mice (n=7) (B6;129-*Gt(ROSA)26Sor*$^{tm4(CAG-GFP*)Nat}$/J) is a conditional *Gt(ROSA)26Sor* (gene trap ROSA 26, Philippe Soriano) knock-in strain. Cre excision of a floxed stop cassette enables CAG promoter-directed GFP expression that is specifically localized to mitochondria via an N-terminal 25 amino acid targeting signal derived from mouse cytochrome c oxidase, subunit VIIIa. A C-terminal V5 epitope tag is

also fused to GFP. Mice containing both Cre Recombinase and GFP-Mito were obtained by breeding mice containing global Cre Recombinase (*The Jackson Laboratory*, Stock No. 003724) with mice containing GFP-Mito (*The Jackson* Laboratory, Stock No. 021429). Tissue samples from the offspring were genotyped by *Transnetyx* (Cordova, TN). Quantitative PCR was performed as follows: 50°C for 2 minutes, 95°C for 10 minutes, followed by 40 cycles of: 95°C for 15 seconds, 60°C for 60 seconds. The final concentration of the forward and reverse primers was 950 nM, the probes at 250 nM, while the DNA was at a concentration of 50–100 ng/μL. The presence of Cre Recombinase was detected using the following: forward primer (TTAATCCATATTGGCAGAACGAAAACG), reverse primer (CAGGCTAAGTGCCTTCTCTACA), and reporter (CCTGCGGTGCTAACC). The presence of the GFP-Mito mutant allele was detected using the following: forward primer (CGTCGTCCTTGAAGAAGATGGT), reverse primer (CACATGAAGCAGCACGACTT), and reporter (CATGCCCGAAGGCTAC). The presence of a GFP-Mito wild type allele was detected using the following: forward primer (TTCCCTCGTGATCTGCAACTC), reverse primer (CTTTAAGCCTGCCCAGAAGACT), and reporter (CCGCCCATCTTCTAGAAAG). Mice containing both global Cre recombinase and the Dendra2 gene were obtained by breeding mice with Cre Recombinase (*The Jackson Laboratory*, Stock No. 003724) with a Dendra2 mouse (*The Jackson Laboratory*, Stock No. 018385). Tissue samples obtained from the mice were genotyped by *Transnetyx* (Cordova, TN). Real-time PCR was performed as follows: 50°C for 2 minutes, 95°C for 10 minutes, followed by 40 cycles of: 95°C for 15 seconds, 60°C for 60 seconds *Transnetyx* (Cordova, TN). The final concentrations for the forward and reverse primers were 900 nM. The Probes were at a final concentration of 250nM *Transnetyx* (Cordova, TN). The presence of the Cre Recombinase allele was detected by using the following: forward primer (TTAATCCATATTGGCAGAACGAAAACG), reverse primer (CAGGCTAAGTGCCTTCTCTACA), and reporter (CCTGCGGTGCTAACC). The presence of the Dendra2 allele was determined using the following: forward primer (GGCGGCGGCCACTA), reverse primer (CACCACCTTCTTGGCCTTGTA), and reporter (CCTGTGCGACTTCAAG).Finally, the detection of the Dendra2 wild type allele was determined using the following: forward primer (TTCCCTCGTGATCTGCAACTC), reverse primer (CTTTAAGCCTGCCCAGAAGACT), and reporter (CCGCCCATCTTCTAGAAAG). All animal experiments were approved by the Cleveland Clinic Institutional Animal Care and Use Committee at Lerner Research Institute in Cleveland, Ohio.

Human subjects

Eleven healthy controls were recruited as part of the Asthma Inflammation Research study (NCT01536522). Patient demographics: 5/6 – female/male; 2/2/7 – Asian/African-American/Caucasian; median age 41.5, range 26–49. All subjects provided informed consent to participate in the study, which was approved by the Cleveland Clinic Institutional Review Board.

MP preparation from mouse blood

Mice were anesthetized with 10% isoflurane and blood was drawn via cardiac puncture. Blood was stored in K_2EDTA tubes on ice and centrifuged at 500g for 5 minutes at 4°C to

collect plasma without deceleration. Approximately 100–200 μL of plasma was collected per mouse. Prostaglandin E1 (PGE1, Sigma P7527) was added to plasma for a final concentration of 10 μM to inhibit activation of any remaining platelets. Plasma was centrifuged at 2,500g for 30 minutes at 4°C to pellet contaminating platelets. Platelet-depleted plasma was collected and centrifuged at 10,000g for 10 minutes at 4°C. Pilot experiments demonstrated this centrifuge speed was sufficient to collect MPs while minimizing damage to mitochondria due to excessive force. MP pellet is not visible so supernatants were collected but 100 μL was left to avoid disturbing the pellet. Tyrode's buffer with 10 μM PGE1 was double-filtered through a 0.1 μm filter. MPs were resuspended after adding 100 μL of the double-filtered Tyrode's buffer with PGE1 to the 100 μL platelet-free plasma with MPs. Thus, MPs were in 50% platelet-depleted plasma during labeling with mitochondrial probes. All MPs were analyzed fresh immediately after isolation.

MP preparation from human blood

Blood was drawn into glass ACD (acid citrate dextrose) tubes and centrifuged without deceleration at 150g for 20 minutes to collect plasma. PGE1 was added to plasma for a final concentration of 10 μM. Plasma was centrifuged without deceleration at 150g for 10 minutes to further clear contaminating red and white blood cells. Plasma was centrifuged at 2,500g for 30 minutes at 4°C to pellet platelets for another study. Platelet-free plasma was collected and centrifuged at 10,000g for 10 minutes at 4°C to pellet MPs. MP pellet is not visible so samples were aspirated down to 100 μL to avoid disturbing the pellet. MPs were resuspended after adding 100 μL of the double-filtered Tyrode's buffer with PGE1 to the 100 μL platelet-free plasma with MPs. Thus, MPs were in 50% platelet-depleted plasma during labeling with mitochondrial probes. All MPs were analyzed fresh immediately after isolation.

MP labeling for flow cytometry

All antibodies and probes were titrated using MPs to determine optimal staining concentrations. Supplemental Figure 1 illustrates positive controls for cell-specific antibodies. Antibodies and probes were prepared at 2X concentrations in double-filtered Tyrode's buffer with PGE1. Antibodies/probe were combined with sample at 1:1 ratio. For surface marker staining MitoTracker Green FM (Invitrogen M7514) staining was done first. Samples were incubated with 250 nM MitoTracker Green for 30 minutes at 37°C. Samples were washed with double-filtered Tyrode's buffer with PGE1 and centrifuged at 10,000g for 10 minutes. Samples were then incubated with antibodies for 30 minutes on ice. Antibodies were used at the following concentrations: anti-human CD41-PECy7 1/200 (BioLegend 303718), anti-human CD45-PE 1/100 (Invitrogen 12-0459-42), anti-human CD144-PE 1/4 (Santa Cruz sc-9989), anti-mouse CD41-PE 1/100 (eBioscience 12-0411-81), anti-mouse CD45-PerCP 1/160 (Invitrogen MA1–10234), and anti-mouse CD144-PECy7 1/50 (eBioscience 25-1441-82). Antibodies and probes were centrifuged at 20,000g for 10 minutes to pellet potential aggregates prior to use. For staining of GFP-mito MPs, samples were incubated with 125 nM MitoTracker Red CMXRos (Invitrogen M7512) at 37°C for 20 minutes. Samples were washed with double-filtered Tyrode's buffer with PGE1 after staining. Presence of true MPs was further validated by dissolving vesicles by treating samples with Triton-X 100. For TMRE (0.4 μM, final concentration) labeling, HBSS with

10 μM PGE1 was used instead of Tyrode's buffer and, where indicated, FCCP was added at a final concentration of 200 μM. The labeling was performed in a 37°C warm water bath and samples were kept warm post-labeling until sample acquisition.

Flow cytometry

GFP-mito MPs and TMRE labeled samples were analyzed on a Fortessa (Becton Dickinson) flow cytometer equipped with 5 lasers (355 nm, 407 nm, 488 nm, 561 nm and 641 nm). The following laser line excitation (Ex) and filters were used: GFP 488 nm Ex., 515/20 filter; MitoTracker Red 488 nm Ex., 710/50 filter, and TMRE 561 nm Ex., 582/15 filter. Surface marker stained MPs were analyzed on an Apogee A50 micro flow cytometer equipped with a 488nm laser. The following filters were used for detection: PerCP 680/35; PE-Cy7 long-pass 740; PE 575/30, and Mitotracker Green 525/50. Apogee Mix Beads (Apogee, #1493) with a refractive index of 1.43, similar to the refractive index of biological samples (1.40) was used for size estimation (29). Rainbow calibration particles (Spherotech RCP-20–5) were used for fluorescence detector calibration between experiments. AbC Total Antibody Compensation Bead kit (Invitrogen A10497) was used for the antibodies and platelets were used for MitoTracker compensation.

Mitochondria transfer into cells and immunoelectron microscopy

Rho-zero HeLa cells (30–32) were cultured in Dulbecco's Modified Eagle Medium-high glucose with 10 mL GLUTAmax, 10% Fetal Bovine Serum, 1% Pen-Strep, 50 μg/mL uridine. Confluent culture of a p100 culture-dish was harvested by trypsinization, washed with PBS, and resuspended in 1 mL culture medium. Wildtype mouse splenocytes were obtained after red blood cell lysis. Circulating peripheral blood micro-particles were isolated from GFP-Mito mice as described above. 100 μL of micro-particles enriched plasma was mixed with the 1 mL Rho-zero cell or splenocytes suspension by gently pipetting up and down for 30 seconds, followed by centrifugation at 500g for 5 minutes. Samples were fixed with 4% PFA, and 0.05% glutaraldehyde overnight in 4°C followed by dehydration with ethanol and then embedded with LR white resin for 6hrs at 50°C until polymerization. Ultrathin section were mounted on nickel grids coated with Forvar. All sections were first incubated overnight with antibody GFP (1:100) followed by a 1hr incubation with a secondary antibody with 10nm gold –conjugated anti rabbit IgG. All grids were then briefly stained with uranyl acetate and lead citrate. Samples were examined with a Tecnai G2 SpiritBT electron microscope operated at 80 kV. Lung mitochondria from Dendra2 mice were isolated as described (33). Transformation of Rho-zero cells were performed as described above and cells were plated overnight before taking fluorescence images. Co-labeling with phagocytosis/endocytosis probe pHrodo red was performed according to manufactures instructions (Thermo Fisher Scientific, Waltham, MA).

Proteomics analysis of circulating mitochondria

Micro-particles obtained from healthy control participants were labeled with TRME. Circulating mitochondria, identified as $TRME^+$ events, were sorted in PBS using a BD Aria II sorter. Circulating mitochondria (counts ~8000) sorted in ~ 560 μL PBS were centrifuged at 16,000g for 30min, the supernatant was removed, and the sample was reconstituted in 6 M urea / 100 mM Tris buffer. The proteins were reduced with DTT and alkylated with

iodoacetamide. After reduction and alkylation, the samples was digested by adding a mixture of Trypsin and Lys-C Mix (Promega # V5071) and incubated 3–4 hours at 37°C. The sample was diluted sixfold with Tris-HCl (pH 8) to reduce urea concentration to less than 1M and digestion was continued overnight at 37°C. The digestion was terminated by adding 1% TFA. The peptide samples were desalted using PepClean C-18 spin columns (Thermo Scientific #89870) and the samples was reconstituted in ~30 μL of 1% acetic acid for LC-MS analysis.The LC-MS system was a ThermoScientific Fusion Lumos tribrid mass spectrometer system. The HPLC column was a Dionex 15 cm × 75 μm id Acclaim Pepmap C18, 2 μm, 100 Å reversed-phase capillary chromatography column. Five μL volumes of the extract were injected and the peptides eluted from the column by an acetonitrile/0.1% formic acid gradient at a flow rate of 0.3 μL/min were introduced into the source of the mass spectrometer on-line. The microelectrospray ion source is operated at 1.9 kV. The digest was analyzed using the data dependent multitask capability of the instrument acquiring full scan mass spectra to determine peptide molecular weights and product ion spectra to determine amino acid sequence in successive instrument scans. The data were analyzed by using all CID spectra collected in the experiment to search the human UniProtKB database with the search programs Sequest bundled in Proteome Discoverer 2.2. The protein and peptide identifications were validated with the program scaffold. The protein FDR rate was set to 1%. Each protein was searched using mitochondrial protein databases, general protein databases, and an extracellular vesicle gene database. Proteins were categorized as *Known Mitochondrial*, *Predicted Mitochondrial and Found in Extracellular Vesicles, and Non-Mitochondrial but Found in Extracellular Vesicles. Known Mitochondrial* proteins were labeled as mitochondrial in all referenced mitochondrial protein databases and the Human Protein Atlas. Proteins labeled *Predicted Mitochondrial and Found in Extracellular Vesicles* were listed in the extracellular vesicle gene database and also predicted to be mitochondrial in at least one of the mitochondrial protein databases or the Human Protein Atlas. Proteins labeled *Non-Mitochondrial but Found in Extracellular Vesicles* were listed as non-mitochondrial in each referenced mitochondrial protein database but found in extracellular vesicles according to the extracellular vesicle gene database

RESULTS

Detection, characterization and imaging of circulating cell-free murine mitochondria

To determine whether intact mitochondria are present in blood circulation, we used flow cytometry to examine MPs in murine platelet-depleted plasma. Flow cytometry is a common method for analyzing MPs, and we followed recommended best practices whenever possible (34,35). Plasma was obtained from wild-type (WT) mice and platelets were depleted via centrifugation. The Apogee Bead Mix (0.1–1 μm) was used to estimate particle size (Fig. 1a). These beads have a refractive index of 1.43 which is similar to the refractive index of MPs (1.40) (29). Platelet-depleted plasma had MPs ranging from 0.1–1 μm, with the small cluster of putative mitochondria falling around 500 nm (Fig. 1b. To determine whether these are in fact mitochondria, we stained platelet-depleted plasma with the mitochondria-specific probe, MitoTracker Green (MT Green) (36). Unstained sample was used to set the gate for MT Green positivity (Fig. 1c). Within the 500 nm cluster, approximately 65% of the particles were MT Green positive (Fig. 1d). We further examined all of the MT Green

positive particles in the platelet-depleted plasma (Fig. 1f) and found approximately 15% of the total MT Green positive particles fell within the 500 nm cluster (Fig. 1g). While the MT Green positive particles ranged in size (Fig. 1g), we decided to take a stringent approach and focus on the 500 nm cluster of mitochondria for the experiments using murine plasma.

To further confirm the presence of circulating mitochondria under physiologic conditions, we analyzed platelet-depleted plasma from transgenic mice with global GFP-labeled mitochondria (GFP-mito) counterstained with MitoTracker Red (MT Red). These samples were analyzed on a BD LSR II flow cytometer which has multiple, higher power lasers allowing for better detection of weak GFP signal and counterstaining with MT Red. Settings were optimized using the Apogee Bead mix (Fig. 2a). We were able to detect particles under 1 μm. However, this cytometer lacks the sensitivity to separate individual populations in this size range so MPs were analyzed as a single population (Fig. 2b). Compared to the unstained WT mouse (Fig. 2c), the stained GFP-mito mouse had approximately 69% double positive particles (Fig. 2f). Additionally, about 26% of the particles were MT Red positive but GFP negative (Fig. 2f). This may be due to loss of the nuclear-encoded GFP signal in some mitochondria. Functional mitochondria have an active respiratory chain and maintain a transmembrane potential which can be quantified by flow cytometry using the specific probe TMRE (36). Circulating mitochondria exhibited substantial retention of TMRE (Fig. 2g). Treatment of the MPs with FCCP, a potent uncoupler of mitochondrial oxidative phosphorylation, dissipated the transmembrane potential, providing further evidence that circulating mitochondria are functionally active. Quantitative measurements of MitoTracker Green and TMRE retention are shown in Table I.

Electron microscopy of circulating mitochondria is challenging because a visible pellet is required for processing. We analyzed whether rho-zero cells could be utilized as carrier-cells for cell-free mitochondria. To test this principle, rho-zero cells were incubated with cell-free lung-derived mitochondria isolated from Dendra2-mice which carry a knocked-in fluorescent protein gene fused with the mitochondrial subunit VIII of cytochrome C oxidase. As a consequence, mitochondria from these mice emits a green fluorescence signal. Rho-zero cells were able to internalize cell-free Dendra2-mitochondria (Fig. 3a–b.). As a negative control, rho-zero cells incubated with buffer only did not show any green fluorescence (Fig. 3b). Next, we analyzed whether we could use cells as a vehicle to visualize circulating mitochondria. MPs isolated from GFP-mito mouse blood were co-incubated with rho-zero cells or wildtype splenocytes, followed by immunoelectron microscopy. As shown in figures 3c,d and e GFP^+ mitochondria were present inside the rho-zero cells or splenocytes. Of note, the fixation process for immunoelectron microscopy doesn't allow perfect preservation of conventional morphology as observed with standard electron microscopy, nevertheless GFP immunoreactivity was clearly detected within mitochondrial structures. In some cells the GFP^+ mitochondria were localized in large vesicles (Fig. 3e). Cells incubated with buffer only did not show any immunoreactivity to GFP (Fig. 3g), confirming the specificity of the staining. Altogether, the results provide multiple lines of evidence that intact and functional mitochondria are present in murine circulation.

MPs are formed through budding of the plasma membrane which subsequently pinches off from the cell. Thus, the MP membrane should contain surface markers from the cell of

origin. To determine the origin of MP enclosed mitochondria, we stained murine platelet-depleted plasma for surface markers of platelets (CD41), vascular endothelial cells (CD144), and leukocytes (CD45). We selected the mitochondria-enriched cluster for analysis (Fig. 4a), gating the MT Green positive population to ensure all particles analyzed contained mitochondria (Fig. 4b). For each marker, the unstained sample was used to set the gate for positivity (Fig. 4c, e, and g). We found approximately 11% of the mitochondria were CD41 positive (Fig. 4d), some of which may be attributable to platelet activation by EDTA as anti-coagulant. Another 11% were CD144 positive (Fig. 4f). However, we found essentially no CD45 positive particles (Fig. 4h). These results indicate that platelets and endothelial cells are a source of circulating mitochondria but leukocytes are not. Additionally, over 75% of the mitochondria were negative for all three markers suggesting they are from another cell type or not enclosed in a MP at all.

Detection and characterization of circulating cell-free human mitochondria

To determine whether cell-free mitochondria are present in humans, we analyzed MPs in platelet-depleted plasma from healthy individuals. When examining the platelet-depleted plasma via flow cytometry, we noted the presence of a few extraneous platelets remaining after depletion (Fig. 5b). To exclude these from our analysis, we used platelet rich plasma to define the platelet population based on size (> 1 μm) (Fig. 5a). This gate was applied to depleted plasma and particles within this gate were excluded from analysis (Fig. 5b). The human plasma did not contain a mitochondria-enriched cluster as seen in the murine plasma, so the entire population of MPs was analyzed together. We stained the MPs for MT Green and used the unstained sample to set the gate for positivity (Fig. 5c). We found approximately 11% of the particles were MT Green positive (Fig. 5d). We stained the plasma for cell surface markers CD41, CD144, and CD45, using the unstained samples to set the gates for positivity (Fig. 5e, g, and i). Amongst the MT Green positive mitochondria, approximately 11% were CD41 positive (Fig. 5f). This was similar to the murine plasma. However, unlike the mice, we found approximately 49% of the mitochondria were CD144 positive (Fig. 5h) and approximately 9% were CD45 positive (Fig. 5j). Interestingly, while humans and mice had similar proportions of platelet-derived mitochondria, humans had more endothelial- and leukocyte-derived mitochondria. To verify that this difference is not due to differences in gating strategies, we applied the gating from the human samples to the mice. Even with analysis of all MT Green positive MPs, the mice had less leukocyte- and endothelial-derived mitochondria compared to the humans, although platelet-derived mitochondria were slightly higher with this strategy (0.25 ± 0.3% $CD45^+$, 11.76 ± 3.2% $CD144^+$, 15.2 ± 8.5% $CD41^+$). As with circulating murine mitochondria, MPs isolated from human circulation were able to retain mitochondria specific TMRE (Fig. 5k). Quantitative measurements of MitoTracker Green and TMRE retention are shown in Table II.

Circulating human mitochondria were sorted based on TMRE positivity for proteomic analysis. A total of 40 proteins were identified (Table I). Among these were nine mitochondria-specific proteins, nine proteins predicted to be found in mitochondria, and twenty-one proteins known to be associated with extracellular vesicles. The results confirm, at a protein level, that circulating mitochondria are present in human blood and suggest that at least a fraction of the mitochondria are within extracellular vesicles.

DISCUSSION

An increasing number of studies have shown that cells release intact mitochondria under conditions of stress, injury, or disease. Here, we've shown intact mitochondria are also released in non-pathologic states and can be detected in the circulation in mice and humans. These mitochondria maintain a transmembrane potential and are able to re-enter cells. The presence of a transmembrane potential suggests that the extracellular mitochondria are intact. The integrity of the mitochondrial genome is a highly sensitive way to assess whether mitochondria are intact, but was not performed here due to limiting samples. Platelets, endothelial cells, and leukocytes all serve as sources of circulating mitochondria, although they did not account for all of the circulating mitochondria. Approximately 77% of the murine and 30% of the human mitochondria were negative for these cell surface markers. This suggests there are other cellular sources of circulating mitochondria. Neurons, astrocytes, fibroblasts, and bone marrow-derived stromal/stem cells (BMSCs) all release intact mitochondria in response to stress or damage (25–27,37,38). Thus, many cell types have the capacity to release mitochondria and may do so in the absence of damage signals. An alternative explanation for the lack of surface markers is release of free mitochondria with no surrounding cell membrane. Activated platelets release free mitochondria (22) and they have also been detected in the circulation of deceased organ donors (28).

Entry of cell-free mitochondria into cells has been described using different terminology including mitochondrial transformation, mitoception, mitochondria transfer, and mitochondria transplantation (39–41). Macropinocytosis, endocytosis and unknown mechanisms have been attributed to entry of extracellular mitochondria into cells (39–41). Our findings show that the ex-vivo mitochondrial transformation of Hela rho-zero cells or splenocytes is a rapid process and independent of phagocytosis/endocytosis. It is also possible that mechanisms of mitochondrial transformation are donor/recipient-cell-dependent. Further studies are required to provide insight this novel concept.

The physiological role of extracellular mitochondria is still unclear. Extracellular mitochondrial components serve as damage associated molecular patterns (DAMPs) which are recognized by pattern recognition receptors (PRRs) on innate immune cells. Thus, extracellular mitochondria may serve to initiate or amplify inflammatory signaling. Indeed, mitochondria activate platelets, neutrophils, macrophages, and dendritic cells *in vitro* (22,26,27). *In vivo*, extracellular mitochondria are correlated with disease severity/adverse events and are associated with increased neutrophil activation and inflammatory cytokines (22,28).

An alternative function of circulating mitochondria may be transfer to cells with dysfunctional mitochondria. Transfer of healthy mitochondria to rescue dysfunctional cells has been demonstrated in a variety of contexts. *In vitro*, BMSC transfer mitochondria to A549 epithelial and endothelial cells with dysfunctional mitochondria, increasing oxygen consumption and ATP production in the recipient cells (42,43). BMSCs also transfer mitochondria *in vivo*. In mouse models of acute lung injury and asthma, BMSC instilled into the lung transfer mitochondria to dysfunctional epithelial cells, restoring ATP production and attenuating disease severity (38,43). Mitochondria are released from BMSC in MPs,

demonstrating the role of MPs in transporting mitochondria between cells (38). However, mitochondrial transfer had only been demonstrated in conditions with cell-to-cell contact. Our data show that circulating mitochondria are able to re-enter cells. It is unknown how long mitochondria maintain their function outside of a cell, as most of the proteins required for mitochondrial function are nuclear-encoded. One study reports function of isolated mitochondria is maintained up to 18 hours after isolation (44). However, this is under optimal conditions *in vitro*. Further studies are needed to determine the exact biological roles of circulating mitochondria. Our findings are in line with a recent publication showing the presence of cell-free and respiratory competent mitochondria in human blood (45). In latter work the number of cell-free mitochondria were estimated, based on mitochondria DNA copy, between 200,000 and 3.7 million per mL human plasma. Our absolute quantification showed a similar range of 822,000 and 2.3 million per mL plasma in humans, and 494,000 and 1.9 million per mL murine plasma. We were unable to obtain a pellet of cell-free mitochondria visible to the naked-eye to process for direct electron microscopy imaging. In the previous work, electron microscopy imaging showed that the cell-free mitochondria were not encapsulated in MPs, while our flow cytometry and proteomics data demonstrate that at least a fraction of the cell-free mitochondria are contained within extracellular vesicles.

Release of intact mitochondria has been described in a number of diseases and inflammatory states. Here we demonstrate the presence of intact and functional mitochondria in the circulation of healthy mice and humans. Characterization of these circulating mitochondria is important, as it defines a baseline in healthy individuals that will allow for comparison in pathological states. Furthermore, it helps to define the physiological relevance of cell-free mitochondria, which gives context to pathological states. As research on extracellular mitochondria expands, defining their origins and functions are important next steps for understanding their overall impact on health and disease.

GEOLOCATION

Cleveland, OH USA

Supplementary Material

Refer to Web version on PubMed Central for supplementary material.

ACKNOWLEDGEMENTS

The authors thank Dr. James McCully (Harvard Medical School) for providing us the rho zero cells and insightful discussion. We also thank the Lerner Research Institute Flow Cytometry Core for assistance with instrument setup, and the Lerner Research Institute Imaging Core for assistance with microscopy.

FUNDING

Supported by NIH grants HL103453, HL081064, HL060917 and HL109250, and the Alfred Lerner Memorial Chair in Innovative Biomedical Research at the Cleveland Clinic. The Fusion Lumos instrument was purchased via an NIH shared instrument grant, 1S10OD023436-01.

References

1. Curtis AM, Edelberg J, Jonas R, Rogers WT, Moore JS, Syed W, and Mohler ER 3rd. (2013) Endothelial microparticles: sophisticated vesicles modulating vascular function. Vasc Med 18, 204–214 [PubMed: 23892447]
2. Melki I, Tessandier N, Zufferey A, and Boilard E (2017) Platelet microvesicles in health and disease. Platelets 28, 214–221 [PubMed: 28102737]
3. Jaimes Y, Naaldijk Y, Wenk K, Leovsky C, and Emmrich F (2017) Mesenchymal Stem Cell-Derived Microvesicles Modulate Lipopolysaccharides-Induced Inflammatory Responses to Microglia Cells. Stem Cells 35, 812–823 [PubMed: 27862694]
4. Laffont B, Corduan A, Ple H, Duchez AC, Cloutier N, Boilard E, and Provost P (2013) Activated platelets can deliver mRNA regulatory Ago2*microRNA complexes to endothelial cells via microparticles. Blood 122, 253–261 [PubMed: 23652806]
5. Skog J, Wurdinger T, van Rijn S, Meijer DH, Gainche L, Sena-Esteves M, Curry WT Jr., Carter BS, Krichevsky AM, and Breakefield XO (2008) Glioblastoma microvesicles transport RNA and proteins that promote tumour growth and provide diagnostic biomarkers. Nat Cell Biol 10, 1470–1476 [PubMed: 19011622]
6. Miranda KC, Bond DT, McKee M, Skog J, Paunescu TG, Da Silva N, Brown D, and Russo LM (2010) Nucleic acids within urinary exosomes/microvesicles are potential biomarkers for renal disease. Kidney Int 78, 191–199 [PubMed: 20428099]
7. Dean WL, Lee MJ, Cummins TD, Schultz DJ, and Powell DW (2009) Proteomic and functional characterisation of platelet microparticle size classes. Thromb Haemost 102, 711–718 [PubMed: 19806257]
8. Thakur BK, Zhang H, Becker A, Matei I, Huang Y, Costa-Silva B, Zheng Y, Hoshino A, Brazier H, Xiang J, Williams C, Rodriguez-Barrueco R, Silva JM, Zhang W, Hearn S, Elemento O, Paknejad N, Manova-Todorova K, Welte K, Bromberg J, Peinado H, and Lyden D (2014) Double-stranded DNA in exosomes: a novel biomarker in cancer detection. Cell Res 24, 766–769 [PubMed: 24710597]
9. Ramachandran S, and Palanisamy V (2012) Horizontal transfer of RNAs: exosomes as mediators of intercellular communication. Wiley Interdiscip Rev RNA 3, 286–293 [PubMed: 22012863]
10. Rhee JS, Black M, Schubert U, Fischer S, Morgenstern E, Hammes HP, and Preissner KT (2004) The functional role of blood platelet components in angiogenesis. Thromb Haemost 92, 394–402 [PubMed: 15269837]
11. Heijnen HF, Schiel AE, Fijnheer R, Geuze HJ, and Sixma JJ (1999) Activated platelets release two types of membrane vesicles: microvesicles by surface shedding and exosomes derived from exocytosis of multivesicular bodies and alpha-granules. Blood 94, 3791–3799 [PubMed: 10572093]
12. Berckmans RJ, Nieuwland R, Boing AN, Romijn FP, Hack CE, and Sturk A (2001) Cell-derived microparticles circulate in healthy humans and support low grade thrombin generation. Thromb Haemost 85, 639–646 [PubMed: 11341498]
13. Oehmcke S, Morgelin M, Malmstrom J, Linder A, Chew M, Thorlacius H, and Herwald H (2012) Stimulation of blood mononuclear cells with bacterial virulence factors leads to the release of pro-coagulant and pro-inflammatory microparticles. Cellular microbiology 14, 107–119 [PubMed: 21951918]
14. Obregon C, Rothen-Rutishauser B, Gitahi SK, Gehr P, and Nicod LP (2006) Exovesicles from human activated dendritic cells fuse with resting dendritic cells, allowing them to present alloantigens. The American journal of pathology 169, 2127–2136 [PubMed: 17148675]
15. Aliotta JM, Sanchez-Guijo FM, Dooner GJ, Johnson KW, Dooner MS, Greer KA, Greer D, Pimentel J, Kolankiewicz LM, Puente N, Faradyan S, Ferland P, Bearer EL, Passero MA, Adedi M, Colvin GA, and Quesenberry PJ (2007) Alteration of marrow cell gene expression, protein production, and engraftment into lung by lung-derived microvesicles: a novel mechanism for phenotype modulation. Stem Cells 25, 2245–2256 [PubMed: 17556595]

16. Nawaz M, Camussi G, Valadi H, Nazarenko I, Ekström K, Wang X, Principe S, Shah N, Ashraf NM, Fatima F, Neder L, and Kislinger T (2014) The emerging role of extracellular vesicles as biomarkers for urogenital cancers. Nature Reviews Urology 11, 688 [PubMed: 25403245]
17. Duarte D, Taveira-Gomes T, Sokhatska O, Palmares C, Costa R, Negrao R, Guimaraes JT, Delgado L, Soares R, and Moreira A (2013) Increased circulating platelet microparticles as a potential biomarker in asthma. Allergy 68, 1073–1075 [PubMed: 23889600]
18. Agouni A, Lagrue-Lak-Hal AH, Ducluzeau PH, Mostefai HA, Draunet-Busson C, Leftheriotis G, Heymes C, Martinez MC, and Andriantsitohaina R (2008) Endothelial dysfunction caused by circulating microparticles from patients with metabolic syndrome. The American journal of pathology 173, 1210–1219 [PubMed: 18772329]
19. Boilard E, Nigrovic PA, Larabee K, Watts GF, Coblyn JS, Weinblatt ME, Massarotti EM, Remold-O'Donnell E, Farndale RW, Ware J, and Lee DM (2010) Platelets amplify inflammation in arthritis via collagen-dependent microparticle production. Science (New York, N.Y.) 327, 580–583
20. Rose JA, Wanner N, Cheong HI, Queisser K, Barrett P, Park M, Hite C, Naga Prasad SV, Erzurum S, and Asosingh K (2016) Flow Cytometric Quantification of Peripheral Blood Cell beta-Adrenergic Receptor Density and Urinary Endothelial Cell-Derived Microparticles in Pulmonary Arterial Hypertension. PLoS One 11, e0156940 [PubMed: 27270458]
21. Hu SS, Zhang HG, Zhang QJ, and Xiu RJ (2014) Circulating CD62P small microparticles levels are increased in hypertension. International journal of clinical and experimental pathology 7, 5324–5326 [PubMed: 25197418]
22. Boudreau LH, Duchez AC, Cloutier N, Soulet D, Martin N, Bollinger J, Pare A, Rousseau M, Naika GS, Levesque T, Laflamme C, Marcoux G, Lambeau G, Farndale RW, Pouliot M, Hamzeh-Cognasse H, Cognasse F, Garraud O, Nigrovic PA, Guderley H, Lacroix S, Thibault L, Semple JW, Gelb MH, and Boilard E (2014) Platelets release mitochondria serving as substrate for bactericidal group IIA-secreted phospholipase A2 to promote inflammation. Blood 124, 2173–2183 [PubMed: 25082876]
23. Hough KP, Trevor JL, Strenkowski JG, Wang Y, Chacko BK, Tousif S, Chanda D, Steele C, Antony VB, Dokland T, Ouyang X, Zhang J, Duncan SR, Thannickal VJ, Darley-Usmar VM, and Deshane JS (2018) Exosomal transfer of mitochondria from airway myeloid-derived regulatory cells to T cells. Redox Biol 18, 54–64 [PubMed: 29986209]
24. Zhang Q, Raoof M, Chen Y, Sumi Y, Sursal T, Junger W, Brohi K, Itagaki K, and Hauser CJ (2010) Circulating mitochondrial DAMPs cause inflammatory responses to injury. Nature 464, 104–107 [PubMed: 20203610]
25. Maeda A, and Fadeel B (2014) Mitochondria released by cells undergoing TNF-alpha-induced necroptosis act as danger signals. Cell Death Dis 5, e1312 [PubMed: 24991764]
26. Zhu M, Barbas AS, Lin L, Scheuermann U, Bishawi M, and Brennan TV (2018) Mitochondria Released by Apoptotic Cell Death Initiate Innate Immune Responses. Immunohorizons 2, 384–397 [PubMed: 30847435]
27. Zhao Z, Zhou Y, Hilton T, Li F, Han C, Liu L, Yuan H, Li Y, Xu X, Wu X, Zhang F, Thiagarajan P, Cap A, Shi FD, Zhang J, and Dong JF (2019) Extracellular mitochondria released from traumatized brains induced platelet procoagulant activity. Haematologica
28. Pollara J, Edwards RW, Lin L, Bendersky VA, and Brennan TV (2018) Circulating mitochondria in deceased organ donors are associated with immune activation and early allograft dysfunction. JCI Insight 3
29. van der Pol E, Coumans FA, Sturk A, Nieuwland R, and van Leeuwen TG (2014) Refractive index determination of nanoparticles in suspension using nanoparticle tracking analysis. Nano Lett 14, 6195–6201 [PubMed: 25256919]
30. 18353857Pacak CA, Preble JM, Kondo H, Seibel P, Levitsky S, Del Nido PJ, Cowan DB, and McCully JD (2015) Actin-dependent mitochondrial internalization in cardiomyocytes: evidence for rescue of mitochondrial function. Biology open 4, 622–626 [PubMed: 25862247]
31. Pacak CA, Preble JM, Kondo H, Seibel P, Levitsky S, Del Nido PJ, Cowan DB, and McCully JD (2015) Actin-dependent mitochondrial internalization in cardiomyocytes: evidence for rescue of mitochondrial function. Biology open 4, 622–626 [PubMed: 25862247]

32. Kukat A, Kukat C, Brocher J, Schafer I, Krohne G, Trounce IA, Villani G, and Seibel P (2008) Generation of rho0 cells utilizing a mitochondrially targeted restriction endonuclease and comparative analyses. Nucleic acids research 36, e44 [PubMed: 18353857]
33. Preble JM, Pacak CA, Kondo H, MacKay AA, Cowan DB, and McCully JD (2014) Rapid isolation and purification of mitochondria for transplantation by tissue dissociation and differential filtration. Journal of visualized experiments : JoVE, e51682 [PubMed: 25225817]
34. Lannigan J, P. Nolan J, and Zucker R (2016) Measurement of extracellular vesicles and other submicron size particles by flow cytometry. Cytometry Part A 89, 109–110
35. Nolan JP, and Duggan E (2018) Analysis of Individual Extracellular Vesicles by Flow Cytometry in Flow Cytometry Protocols (Hawley TS, and Hawley RG eds.), Springer New York, New York, NY pp 79–92
36. Cottet-Rousselle C, Ronot X, Leverve X, and Mayol JF (2011) Cytometric assessment of mitochondria using fluorescent probes. Cytometry A 79, 405–425 [PubMed: 21595013]
37. Hayakawa K, Esposito E, Wang X, Terasaki Y, Liu Y, Xing C, Ji X, and Lo EH (2016) Transfer of mitochondria from astrocytes to neurons after stroke. Nature 535, 551–555 [PubMed: 27466127]
38. Islam MN, Das SR, Emin MT, Wei M, Sun L, Westphalen K, Rowlands DJ, Quadri SK, Bhattacharya S, and Bhattacharya J (2012) Mitochondrial transfer from bone-marrow-derived stromal cells to pulmonary alveoli protects against acute lung injury. Nat Med 18, 759–765 [PubMed: 22504485]
39. Kesner EE, Saada-Reich A, and Lorberboum-Galski H (2016) Characteristics of Mitochondrial Transformation into Human Cells. Scientific reports 6, 26057 [PubMed: 27184109]
40. Caicedo A, Fritz V, Brondello JM, Ayala M, Dennemont I, Abdellaoui N, de Fraipont F, Moisan A, Prouteau CA, Boukhaddaoui H, Jorgensen C, and Vignais ML (2015) MitoCeption as a new tool to assess the effects of mesenchymal stem/stromal cell mitochondria on cancer cell metabolism and function. Scientific reports 5, 9073 [PubMed: 25766410]
41. Cowan DB, Yao R, Thedsanamoorthy JK, Zurakowski D, Del Nido PJ, and McCully JD (2017) Transit and integration of extracellular mitochondria in human heart cells. Scientific reports 7, 17450 [PubMed: 29234096]
42. Spees JL, Olson SD, Whitney MJ, and Prockop DJ (2006) Mitochondrial transfer between cells can rescue aerobic respiration. Proc Natl Acad Sci U S A 103, 1283–1288 [PubMed: 16432190]
43. Ahmad T, Mukherjee S, Pattnaik B, Kumar M, Singh S, Kumar M, Rehman R, Tiwari BK, Jha KA, Barhanpurkar AP, Wani MR, Roy SS, Mabalirajan U, Ghosh B, and Agrawal A (2014) Miro1 regulates intercellular mitochondrial transport & enhances mesenchymal stem cell rescue efficacy. EMBO J 33, 994–1010 [PubMed: 24431222]
44. Lanza IR, and Nair KS (2009) Functional assessment of isolated mitochondria in vitro. Methods in enzymology 457, 349–372 [PubMed: 19426878]
45. Al Amir Dache Z, Otandault A, Tanos R, Pastor B, Meddeb R, Sanchez C, Arena G, Lasorsa L, Bennett A, Grange T, El Messaoudi S, Mazard T, Prevostel C, and Thierry AR (2020) Blood contains circulating cell-free respiratory competent mitochondria. FASEB journal : official publication of the Federation of American Societies for Experimental Biology

HIGHLIGHTS

Extracellular Mitochondria in blood:

- Originate from hematopoietic and nonhematopoietic cells.
- Are encapsulated in extracellular vesicles.
- Have an active transmembrane potential.
- Are able to enter cells.

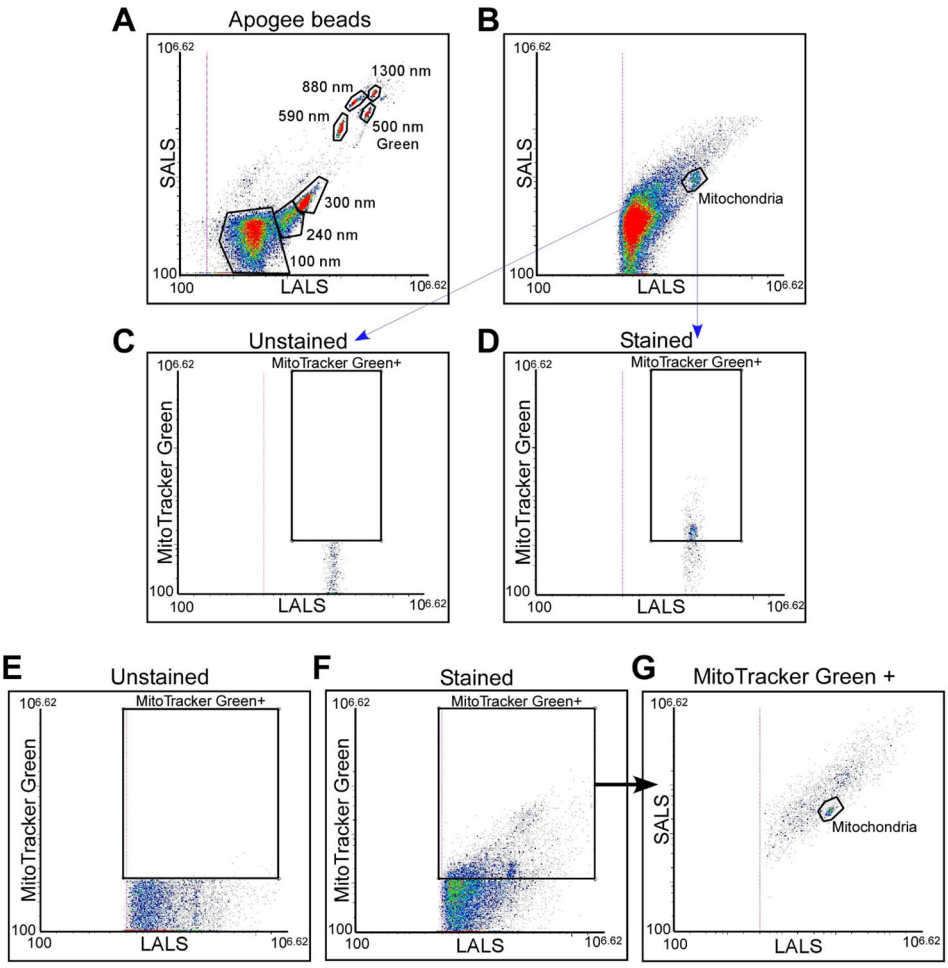

Figure 1: Murine circulating MPs stain positive for mitochondria probe MitoTracker Green.

(A) Apogee Beads Mix (100–1300 nm) was used to estimate relative particle size. (B) LALS vs. SALS plot of murine platelet-depleted plasma MPs. The cluster of putative mitochondria around 500 nm. This population stained positive for MT Green (D) compared to unstained (C). (E) Ungated, unstained MPs were used to set a positive gate for MT Green. (F) All MT Green positive particles were plotted on the LALS vs. SALS plot (G). Plots are representative images, n=10.

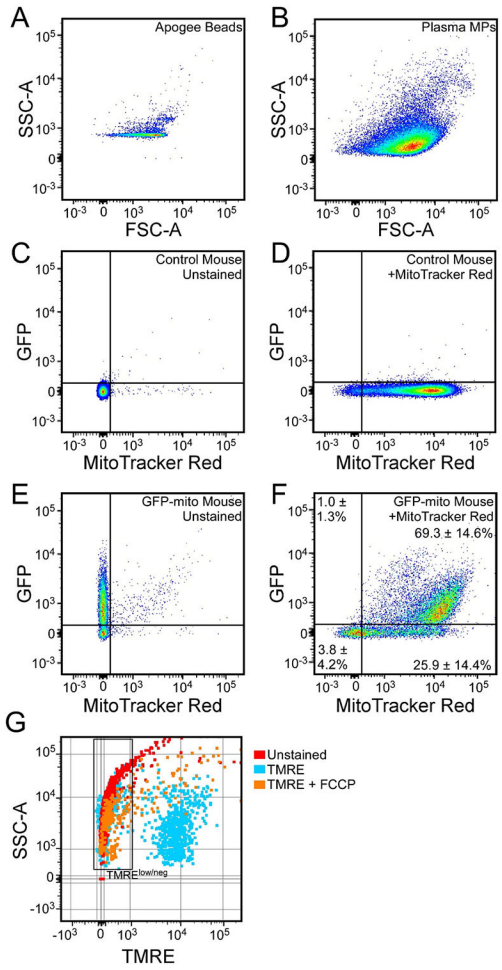

Figure 2: Mitochondria-specific GFP in MPs and mitochondria-specific TMRE retention.

Samples were run on a BD LSR II flow cytometer to analyze co-labeling of mitochondria-targeted GFP expression and MitoTracker Red. (A) Apogee beads were used to determine the settings to detect submicron particles. 500 nm beads gated based on green fluorescence are shown in red. (B) Plasma MPs were detectable with these settings. (C) MPs from an unstained, WT mouse were used to set the gates for MT Red and GFP positivity. (D) MPs from a WT mouse stained positive for MT Red. (E) Unstained MPs from GFP-mito mice were GFP positive. (F) MT Red stained MPs from GFP-mito mice were double positive for GFP and MT Red. (G) Mitochondria-specific TMRE retention in MPs from WT mice. Plots are representative images, percentages represent mean ± SD, n=7.

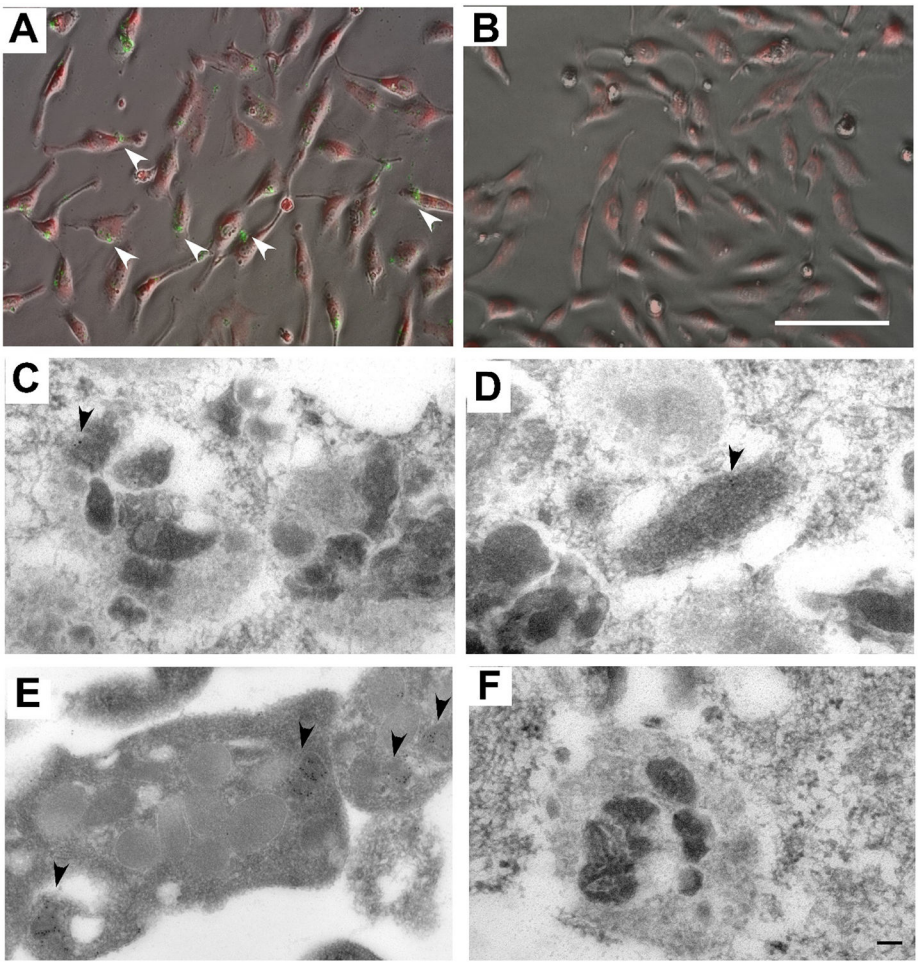

Figure 3: Electron microscopic imaging of circulating mitochondria.

Rho-zero HeLa cells were used as carriers for circulating mitochondria. (A) Proof of principle that rho-zero cells were able to uptake cell-free mitochondria genetically tagged with green fluorescence (white arrows). (B) Cells incubated with buffer only. Scale-bar = 150 μm. (C-D) Immunoelectron microscopic imaging of circulating GFP-mitochondria incorporated into rho-zero cells (C-D) or splenocytes (E). The figures showed low contrast by design to minimize antigen loss within the tissue as well as obtain more specific immunogold labeling for electron microscopy. We used a protocol with low fixative concentration direct dehydration and embedding, without post-fixation using osmium tetroxide. As a result, the images showed low-contrast due to the milder fixation protocol employed in order to maximally protect the antigenicity of the tissue. Thus, the samples were not preserved as well as conventional electron microscopy. Black arrows point to dense black dots of GFP immunoreactivity in mitochondria. (F) Cells incubated with buffer only were negative. Scale-bar = 100 nm.

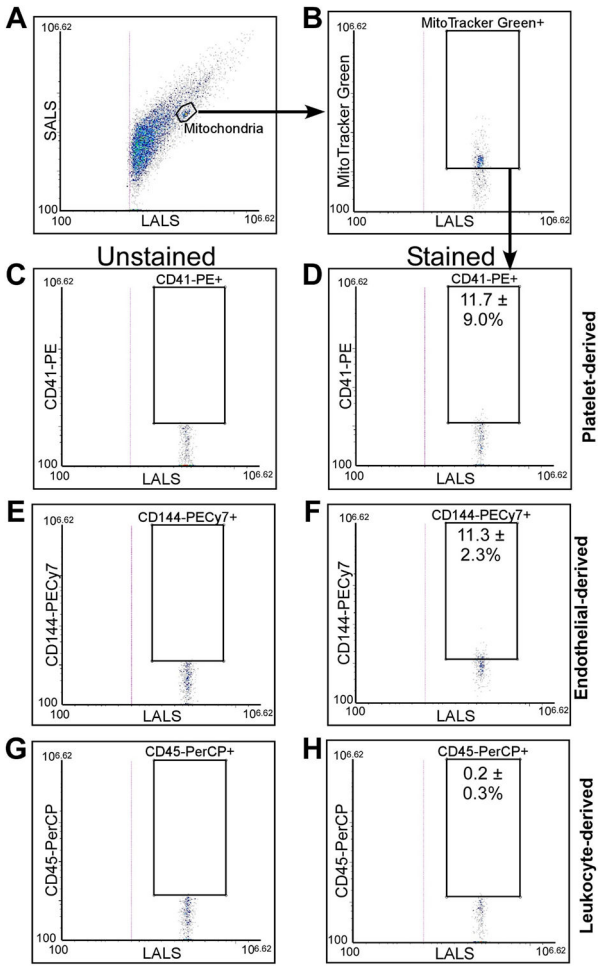

Figure 4: Murine circulating mitochondria stain positive for CD41 and CD144 but not CD45.

Mitochondria were gated based on size (A), then based on MT Green staining (B). The resulting population was then analyzed for CD41-PE staining (D), CD144-PECy7 staining (F), and CD45-PerCP staining (H). Percentages represent the mean ± SD % positive for the respective stain. Positive gates were set based on unstained samples (C, E, G). Plots are representative images, n=10.

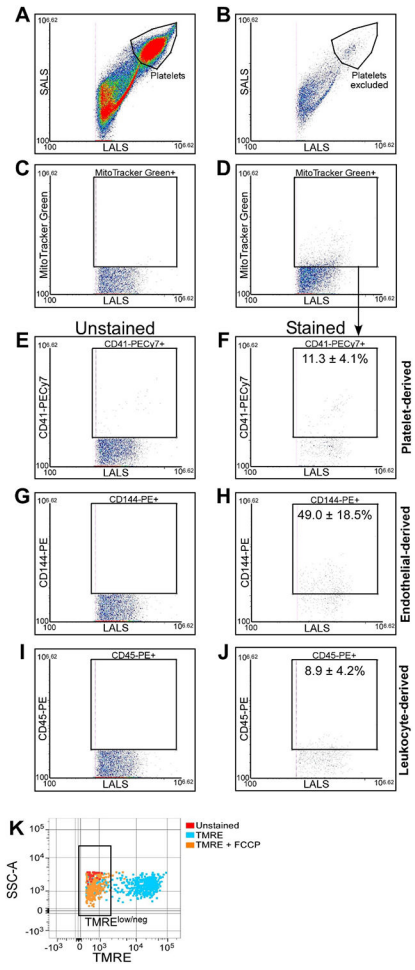

Figure 5: Human circulating mitochondria stain positive for CD41, CD144, and CD45, and retain TMRE.

Platelets were gated based on size in the platelet-rich plasma samples (A). This gate was used to exclude extraneous platelets from the platelet-depleted plasma (B). MT Green positive gate was set based on the unstained sample (C). MT Green positive particles were selected (D) and the resulting population was then analyzed for CD41-PECy7 staining (F), CD144-PE staining (H), and CD45-PE staining (J). Percentages represent the mean ± SD % positive for the respective stain. Positive gates were set based on unstained samples (E, G, I). (K) Mitochondria-specific TMRE retention in MPs. Plots are representative images, n=5.

Table I.

Quantification of MitoTracker and TMRE retention in Murine Platelet-Depleted Plasma.

Values denote Mean ± SE. Absolute number of MPs/mL plasma were obtained from the Apogee flow cytometer and multiplied by two to correct for dilution. Gating of TRME $^{low/neg}$ in shown in Figure 2G.

Measurement	Murine
MitoTracker^{+} MPs (%)	4.1 ± 1.8
MitoTracker^{+} MPs (10^6/mL plasma)	0.93 ± 0.33
TMRE (MFI 10^3)	5.9 ± 4.5
TMRE $^{low/neg}$ inTMRE labeling (%)	33.0 ± 5.9
TMRE $^{low/neg}$ in [TMRE + FCCP] labeling (%)	63.2 ± 2.8

Table II.

Quantification of MitoTracker and TMRE retention in Human Platelet-Depleted Plasma.

Values denote Mean ± SE. Absolute number of MPs/mL plasma were obtained from the Apogee flow cytometer and multiplied by two to correct for dilution. Gating of TRME $^{low/neg}$ in shown in Figure 5K.

Measurement	Human
MitoTracker^{+} MPs (%)	11.0 ± 1.3
MitoTracker^{+} MPs (10^6/mL plasma)	1.4 ± 0.26
TMRE (MFI 10^3)	3.4 ± 2.4
TMRE $^{low/neg}$ inTMRE+ gate (%)	32.0 ± 7.8
TMRE $^{low/neg}$ in [TMRE + FCCP]$^{+}$ gate (%)	86.8 ± 7.4

Table III.

Summary of proteins identified in isolated circulating mitochondria samples.

These mitochondria samples were digested with trypsin and the digests were analyzed by LCMS/MS on a Fusion Lumos instrument. Protein identifications were performed by searching the data against the human SwissProtKB database with the program PD 2.2. Protein and peptide validations were performed with the program Scaffold to an FDR rate of < 1%.

Known Mitochondrial Proteins	**Accession**	**Gene**	**Mass**	**Pep**	**Seq. Cov**	**PSMs**	**NSAF**
Mitochondrial fission factor	Q9GZY8	MFF	38	8	37.0%	39	0.0719
ATP synthase subunit beta, mitochondrial	P06576	ATP5F1B	57	4	9.5%	5	0.00596
60 kDa heat shock protein, mitochondrial	P10809	HSPD1	61	2	4.2%	2	0.0022
ATP synthase subunit alpha, mitochondrial	P25705	ATP5F1A	60	6	7.4%	6	0.00684
Predicted Mitochondrial and found in extracellular vesicles	**Accession**	**Gene**	**Mass**	**Pep**	**Seq. Cov**	**PSMs**	**NSAF**
Heat shock protein HSP 90-beta	P08238	HSP90AB1	83	10	20.0%	13	0.0113
Glyceraldehyde-3-phosphate dehydrogenase	P04406	GAPDH	36	6	20.0%	6	0.0113
Pyruvate kinase PKM	P14618	PKM	58	6	12.0%	6	0.00712
Peroxiredoxin-2	P32119	PRDX2	22	2	5.6%	3	0.00955
Triosephosphate isomerase	P60174	TPI1	31	2	4.5%	2	0.00441
Heat shock cognate 71 kDa protein	P11142	HSPA8	71	4	3.6%	7	0.00683
Tubulin alpha-1A chain	Q71U36	TUBA1A	50	4	12.0%	7	0.00978
Actin, cytoplasmic 1	P60709	ACTB	42	4	37.0%	9	0.0151
Vimentin	P08670	VIM	54	4	9.9%	4	0.00541
Caspase-14	P31944	CASP14	28	3	15.0%	5	0.013
Annexin A2	P07355	ANXA2	39	2	2.7%	2	0.00372
Non-mitochondrial but found in extracellular vesicles	**Accession**	**Gene**	**Mass**	**Pep**	**Seq. Cov**	**PSMs**	**NSAF**
Myosin-6	P13533	MYH6	224	24	16.0%	28	0.0091
Serum albumin	P02768	ALB	69	21	31.0%	28	0.029
Actin, alpha cardiac muscle 1	P68032	ACTC1	42	15	47.0%	22	0.0368
Hemoglobin subunit beta	P68871	HBB	16	6	38.0%	9	0.0386
Hemoglobin subunit alpha	P69905	HBA1	15	5	28.0%	9	0.0399
Creatine kinase B-type	P12277	CKB	43	4	10.0%	4	0.00662
Tropomyosin alpha-1 chain	P09493	TPM1	33	5	17.0%	5	0.0111
Myosin light chain 4	P12829	MYL4	22	4	31.0%	5	0.016
Histone H2A type 1-A	Q96QV6	HIST1H2AA	14	4	22.0%	7	0.0337
Histone H2B type 1-K	O60814	HIST1H2BK	14	3	26.0%	5	0.025
Elongation factor 1-alpha 1	P68104	EEF1A1	50	3	9.70%	5	0.00682
Fructose-bisphosphate aldolase A	P04075	ALDOA	39	3	12.0%	4	0.00692
Histone H4	P62805	HIST1H4A	11	4	21.0%	4	0.0245
Filamin-A	P21333	FLNA	281	3	1.0%	3	0.000714

Myoglobin	P02144	MB	17	3	29.0%	4	0.0164
Myosin-7	P12883	MYH7	223	2	15.0%	3	0.000977
L-lactate dehydrogenase A chain	P00338	LDHA	37	2	5.7%	2	0.0038
Versican core protein	P13611	VCAN	373	3	0.29%	3	0.000557
Histone H1.4	P10412	HIST1H1E	22	3	12.0%	3	0.00863
Eukaryotic translation initiation factor 2 subunit 3	P41091	EIF2S3	51	2	7.4%	2	0.00267
Histone H3.1	P68431	HIST1H3A	15	2	26.0%	3	0.0139
Protein-glutamine gamma-glutamyltransferase E	Q08188	TGM3	77	2	2.9%	2	0.00182
Biglycan	P21810	BGN	42	2	6.8%	2	0.00342
Zinc-alpha-2-glycoprotein	P25311	AZGP1	34	2	3.4%	2	0.00423
Tubulin beta chain	P07437	TUBB	50	2	3.4%	2	0.00284
Protein Used in Digestion during Sample Prep	**Accession**	**Gene**	**Mass**	**Pep**	**Seq. Cov**	**PSMs**	**NSAF**
Lysyl endopeptidase	Q02SZ7	prpL	48	15	36.0%	184	0.0219

Accession: protein accession number. Pep: Number of peptides identified for each protein. Seq Cov: The total protein sequence identified by the observed peptides. PSM's: Total number of spectra identified for each proteins. NSAF: Normalized spectral abundance factor-protein spectral counts normalized to total spectral counts identified in the sample and length of the protein.